26th ABCM International Congress of Mechanical Engineering
November 22-26, 2021. Florianópolis, SC, Brazil

COB-2021-0422
EVALUATION OF NONLINEAR MODES OF A 2 DOF OSCILLATOR USING POINCARÉ MAP

Filipe Eduard Leite Ossege
Aline Souza de Paula
University of Brasília, Department of Mechanical Engineering, 70.910-900, Brasília, DF
eduard.ossege@gmail.com
alinedepaula@unb.br

Abstract. *The dynamics of nonlinear systems is crucial for the understanding of real life's phenomena, since most of the dynamical systems given by nature are described by nonlinearities. Linear systems have normal modes that are orthogonal to each other. One way to define these modes is by synchronous time response of all degrees-of-freedom. In a similar way, nonlinear systems possess nonlinear modes. But, in contrast with linear systems, they are not normal and because of this they can be coupled. In such way, non excited frequencies can appear in the system 's response, an unexpected behavior, due to nonlinear modes coupling. Understanding the nonlinear modes is a crucial role, as they described the system in a state that, with excitation, can lead to the breaking of the physical components of the machinery. Because of this, it is important to avoid the excitation of nonlinear modes, in order to prevent accidents in engineering projects and not to bear with avoidable costs. In this work, a nonlinear system with two degrees-of-freedom under free vibrations is studied using an numerical approach, based on the Poincaré map, that highlights the modes by singular points on a graph. The nonlinearity is provided by 3 nonlinear stiffness elements, represented by springs with cubic terms. The nonlinear modes for different values of stiffness and energy are obtained. The main objective of this paper is the identification of the nonlinear modes of this system by means of a numerical method, the Poincaré section, that does not require the extensive calculation of the analytic solution. The stability of the nonlinear modes is also analyzed. The obtained results are the identification of modes and how the variation of the system's parameters, such as energy, changes the quantity of modes and their stability. The main conclusion is that this technique can be used for the identification of nonlinear modes without the need of extensive calculations.*

Keywords: *nonlinear dynamics, nonlinear vibration, linear normal modes, nonlinear modes, Poincaré map*

1. INTRODUCTION

Nonlinear dynamics have fascinated scientists for many years. The majority of problems presented by nature are described by complicated nonlinear phenomena, such as celestial bodies problem (Krishnaswami and Senapati, 2019), weather prediction (Bengtsson *et al.*, 1981), insect population growth (Costantino *et al.*, 1997) and molecular simulation of the human body (Dinicola *et al.*, 2011). Nonlinear systems possess complicated behavior, since analytical solutions can not be usually found in most cases. For this reason, different tools were developed in order to present information of these systems, such as qualitative and quantitative methods.

In this work, a specific response is studied: the Nonlinear Mode (NM). It represents a synchronous and periodic motion from all Degrees-of-Freedom (DOFs) of the system (Rosenberg, 1962). When excited, the system presents a critical behavior under modal motion, which can compromise the integrity of the system's structure. Hence, modes can be used in structural health monitoring (Kerschen *et al.*, 2009).

Month and Rand (1980) show a method for obtaining the Poincaré map using the first integrals of a system, more specifically, the total energy and the in-phase mode energy. As an example, they applied the methodology to a linear system. Vakakis and Rand (1992a) present the Poincaré map of a nonlinear system with nonlinear stiffness for low energies and identify the NMs for this case. Vakakis and Rand (1992b) studied the same system, but for high energies, instead. Under this condition, the system presented a chaotic like motion, identified by the format of the Poincaré map. In this work, the same system analyzed by Vakakis and Rand (1992a) and Vakakis and Rand (1992b) is investigated. Then, a parametric analysis of the nonlinear stiffness constants is evaluated, considering different levels of energy and showing the influence in the quantity of modes and the type of stability.

2. NONLINEAR MODE

There are several definitions of a NM in the literature (Kerschen *et al.*, 2009). For example, Shaw and Pierre (1993) define a nonlinear mode as an invariant manifold in the phase space. Such concept can be applied directly to systems with dissipative elements. Another definition is made by by Rosenberg (1962), who defined a mode as a synchronous and periodic motion from all DOFs of a system. On the other hand, the nonlinear mode from Rosenberg (1962) can not be applied directly to dissipative systems. In this work, the definition of Rosenberg (1962) is regarded, such that a system under modal motion has the properties:

1. All DOFs reach their equilibrium position at the same time, more specifically, t_0,
2. All DOFs vibrate with the same frequency, in other words, their displacement are periodic functions with the same period, T,
3. The displacement of all DOF can be described as a single variable function which depends only on the displacement of one arbitrary DOF. For a linear system, this function is a linear function, which means that the ratio of the displacement of any one DOF to that of any other is equal to a constant.

The 3 conditions established by Rosenberg (1962) for a NM are given respectively by

$$\begin{aligned} &u_i(t_0) = 0, \\ &u_i(t) = u_i(t+T), \\ &u_i = u_i(u_k), \end{aligned} \tag{1}$$

where u_i is the displacement of the i-th DOF when the system is under the motion of a NM, t is the time, t_0 is a specific time where all DOFs reach the equilibrium point (displacements equal zero), T is the period of the NM and u_k is the displacement of the k-th DOF arbitrarily chosen for evaluating the function.

The modes of a linear system play an important role, since they can be used to find the response of free vibration of any linear system, with the linear combination of the system's modes (Rosenberg, 1966). For linear systems, there is a property that the number of modes is equal to the number of DOFs. Besides that, it is possible to define an orthogonality between these linear modes. As a result, some works call linear modes as normal modes.

However, for a nonlinear system, the superposition principle is not valid. As a consequence, it is not possible to use modes to find the response of a free vibration nonlinear system and even the number of modes is not always equal to the number of DOFs. Furthermore, the modes from nonlinear systems are not orthogonal, so that the expression “normal mode” should not be applied in this case. Even so, some articles use the term “nonlinear normal mode”, due to the habit acquired in linear systems (Gonçalves, 2012). In this work, to avoid confusion, the modes from nonlinear systems are not called normal.

3. METHODOLOGY

In order to simulate the system, a numeric method for solving differential equations is applied. In this work, the Runge-Kutta 4th order method is used in order to obtain the system's time response numerically, due to its high precision compared with methods such as implicit or explicit Euler and Runge-Kutta of lower order. The initial conditions are chosen with respect to the first integrals of the system, i.e., variables that are conserved with the evolution of time, for example, the total energy.

3.1 Poincaré Section

With the time response for multiple cases obtained, a qualitative method is used for identifying which one of them is actually a NM. The approach is based on the Poincaré section, which consists of a phase space portrait on every time the solution of the system reaches a certain value.

The Poincaré map is a technique from which one can transform a continuous system in a discrete system. Within this process, the dimension of the problem is reduced, thus, the analysis of the problem becomes simpler than the one with the continuous system (Savi, 2006). There is no general method for constructing a Poincaré map, since in every system the section is obtained in a different way. To obtain the Poincaré map, one must define a surface that is transverse to the flow of the state variables. As time goes on, the solution travels in phase space and crosses this surface. The place where the solution has crossed the surface is stamped with a dot. This continues until a sufficient number of points is obtained. Hence, from the continuous system, only discrete points, that were stroboscopically acquired, are observed in the map. The surface itself is called Poincaré section, while the surface filled with points is called Poincaré map.

One can note that, since a numerical method is used to obtain the solution, the solution itself is not continuous, but discrete. So, it is possible that the intersection between the solution and the Poincaré surface occurs between 2 discrete values of the solution, which can lead to errors for the construction of the map. This error is not so much significant, so, in this work, the first value before the Poincaré section is selected to be part of the map.

In this work, the section plane is the same one used by Vakakis and Rand (1992a) and Vakakis and Rand (1992b) for a 2 DOFs system. The cutting plane is given by

$$\Sigma = \{u_1 = 0, v_1 > 0\} \cap \{H = h\}, \tag{2}$$

where Σ is the Poincaré section, u_1 is the displacement of the first DOF, $v_1 = \dot{u}_1$ is the velocity of the first DOF, being the dot superscript a time derivative, $\cap$ is the intersection symbol, H is the Hamiltonian of the system or the total energy and h is a constant or the level curve of the Hamiltonian.

At Eq. (2), the term $H = h$ represents that the total energy of the system is conserved, i.e., constant. This condition is guaranteed by the governing equations and the value of h is given by the initial conditions. The Poincaré map acquisition begins with selecting the values of the solution that contain $u_1 = 0$ and $v_1 > 0$ at the same time. The Poincaré section must preserve orientation. For that manner, the map can only be stamped with a dot when the solution crosses the front area of the surface. If the solution crosses the surface in the opposite direction, in other words, the back area of the surface, the map must not be stamped. This condition is well represented by the term $v_1 > 0$, which guarantees the preservation of orientation in the section.

Figure 1 illustrates the crossing process of the solution with the Poincaré section. The points A and A' must be represented or stamped in the Poincaré map, while the point B must be ignored, since the latter has intercepted the Poincaré surface in a opposite direction.

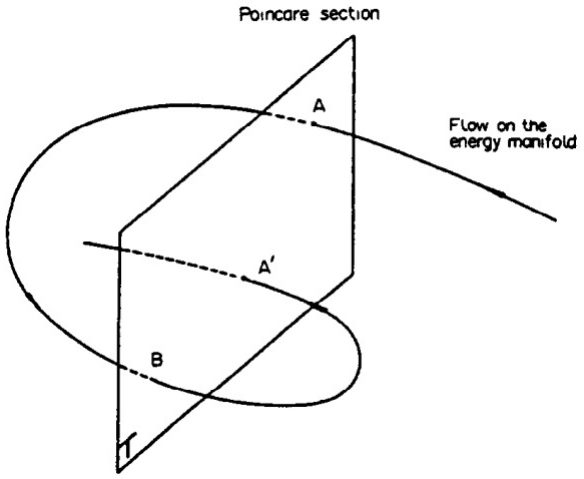

Figure 1: Representation of the solution crossing the Poincaré section. (Vakakis and Rand, 1992a)

The qualitative identification of modes is given by the map 's format. Both the NMs and their stability are recognized with the map, since a fixed point represents a stable NM and a saddle point is an unstable NM. Besides that, it is possible to indicate a chaotic behavior, if a dense region of points apparently without order appears. Since this is a qualitative method, one can not be certain of the system 's behavior (chaotic, quasi-periodic or periodic). To be certain of this, one must use a quantitative method.

Figure 2 shows an example of NMs identification, using the definition of NM from Rosenberg (1962). At the map from the left corner, there are 4 NMs: 3 stable, each represented by a single point, and 1 unstable, given by the intersection of the map with itself. At the map from the center, there are 2 modes only, in other words, the unstable mode from the left map has become stable and the 2 stable modes have vanished. At the map from the right corner, there are 4 modes once again: 3 stables and 1 unstable, due to the bifurcation of the stable NM from the center map.

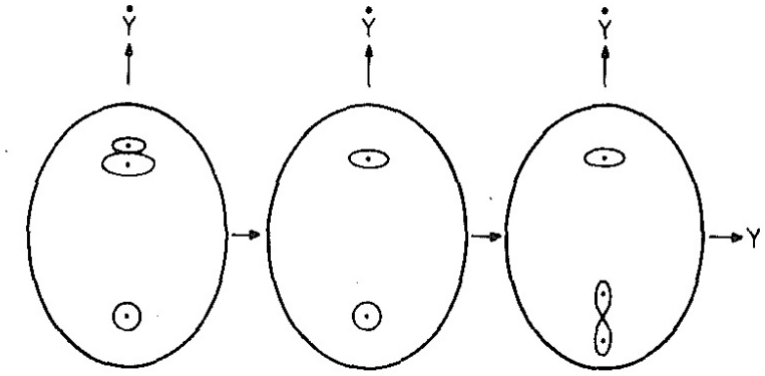

Figure 2: Evolution of the Poincaré map due to the variation of certain parameter (Month and Rand, 1980).

4. DYNAMICAL SYSTEM

Figure 3 shows the nonlinear system with 2 DOFs, 2 standard springs and 3 cubic springs, the same system used by (Vakakis and Rand, 1992a) and (Vakakis and Rand, 1992b).

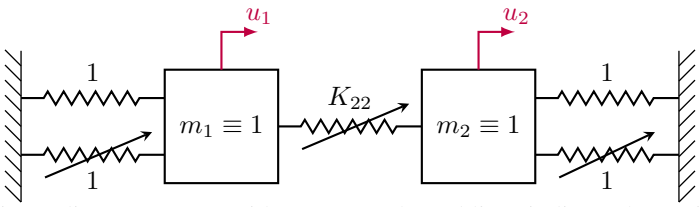

Figure 3: Spring-mass nonlinear discrete system with 2 DOFs. The red lines indicate the positive reference arbitrated for the DOFs.

At Fig. 3, u_1 and u_2 are the displacement of the first and second DOF, respectively. Both masses, m_1 and m_2, are assumed to be unitary. The linear stiffness is represented by a zigzag line, while the cubic stiffness is represented by the same line covered with an arrow (Kerschen *et al.*, 2009). The anchor springs have unitary stiffness, while the middle spring has the constant K_{22} as the value of cubic stiffness. If a new value of K_{22} is considered, a new system is obtained. All the variables used in this work are dimensionless, concerning the work of Vakakis and Rand (1992a) and Vakakis and Rand (1992b).

In order to obtain the governing equations of the system, the Newton method is used. Figure 4 displays the Free Body Diagram (FBD) of each mass.

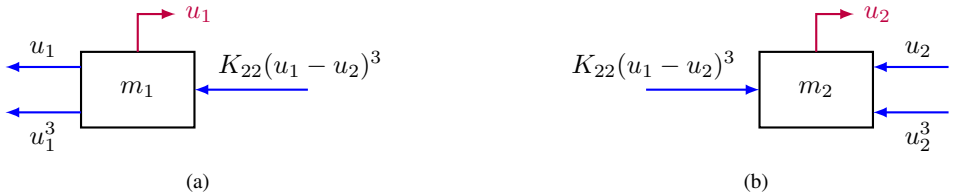

Figure 4: FBDs from the nonlinear system. The blue lines show the forces under each mass, while the red lines indicate the positive reference arbitrated for the DOFs. (a) Left body e (b) Right body.

For the first mass, applying Newton's second law at Fig. 4a, one obtains

$$-(u_1 + u_1^3) - K_{22}(u_1 - u_2)^3 = m_1 \ddot{u}_1, \tag{3}$$

where $\ddot{u}_1$ is the second time derivative from the first DOF displacement, u_1.

For the second mass, applying Newton's second law at Fig. 4b leads to

$$K_{22}(u_1 - u_2)^3 - (u_2 + u_2^3) = m_2 \ddot{u}_2. \tag{4}$$

Thus, considering the masses as unitary, the governing equations are

$$\begin{cases} \ddot{u}_1 + u_1 + u_1^3 + K_{22}(u_1 - u_2)^3 = 0 \\ \ddot{u}_2 + u_2 + u_2^3 + K_{22}(u_2 - u_1)^3 = 0. \end{cases} \tag{5}$$

The system's total energy is conserved, since there is no inclusion of dissipative terms in Eq. (5).

4.1 Equivalence between Initial Conditions and First Integrals

In order to analyze different solutions of the system, it is necessary to find its first integrals. Sastry (2013) defines first integral as a function g such that

$$\frac{\mathrm{d}g}{\mathrm{d}t} = \dot{g} = 0, \tag{6}$$

in other words, for all time, the value g is conserved. One of the first integrals is the total energy of the system, given by

$$H(u_1, u_2, v_1, v_2) = \frac{1}{2}\left(v_1^2 + v_2^2\right) + \frac{u_1^2}{2} + \frac{u_1^4}{4} + K_{22}\frac{(u_1 - u_2)^4}{4} + \frac{u_2^2}{2} + \frac{u_2^4}{4} = h, \tag{7}$$

where H is the Hamiltonian, h is a constant, u_1 and u_2 are the displacements of the first and second DOF, respectively, and v_1 and v_2 are their velocities.

Month and Rand (1980) show another first integral for a linear system: the in-phase mode energy, given by

$$C(u_1, u_2, v_1, v_2) = \frac{1}{4}(v_1 + v_2)^2 + \frac{1}{4}(u_1 + u_2)^2 = c, \tag{8}$$

where C is the in-phase mode energy and c is a constant that represents the level curve from C. Although being a first integral for a linear system in the paper of Month and Rand (1980), this variable is used in this work. For this case, if the in-phase mode energy is equal to the total energy, h, the system presents a in-phase mode. If the in-phase mode energy is minimum, i.e., equals to zero, the system presents a anti-phase mode.

Let u_{10} and u_{20} be the initial conditions of displacement for the first and second DOF, respectively, and v_{10} and v_{20} be the initial conditions of velocity for the first and second DOF. The values $u_{10} = 0$ e $u_{20} = 0$ are arbitrated, such that,

$$\begin{cases} H(0, 0, v_{10}, v_{20}) = \dfrac{1}{2}(v_{10}^2 + v_{20}^2) = h \\ C(0, 0, v_{10}, v_{20}) = \dfrac{1}{4}(v_{10} + v_{20})^2 = c \end{cases} \implies \begin{cases} v_{10}^2 + v_{20}^2 = 2h \\ (v_{10} + v_{20})^2 = 4c. \end{cases} \tag{9}$$

Equation (9) represents an algebraic nonlinear system with 2 equations and 2 variables. Since it is a quadratic system, one can conclude that there are two possible answers. One of them is given by the variable c_1,

$$\begin{cases} v_{10} = \sqrt{c_1} + \sqrt{h - c_1} \\ v_{20} = \sqrt{c_1} - \sqrt{h - c_1}. \end{cases} \tag{10}$$

The last possibility is given by the variable c_2, such that

$$\begin{cases} v_{10} = \sqrt{c_2} - \sqrt{h - c_2} \\ v_{20} = \sqrt{c_2} + \sqrt{h - c_2}. \end{cases} \tag{11}$$

Because v_{10} and v_{20} are real values variables, one can note from Eqs. (10) and (11) that $c \geq 0$ and $c \leq h$. Hence, the domain of c is

$$0 \leq c \leq h. \tag{12}$$

5. RESULTS

Concerning the boundary of the Poincaré map, represented by a black line which the map never reaches, it is used

$$2h = \frac{1}{2}\left(1 + K_{22}\right) u_2^4 + u_2^2 + \dot{u}_2^2, \tag{13}$$

following the work of Vakakis and Rand (1992a).

5.1 First Case ($K_{22} = 0.01$)

Figure 5 shows the Poincaré map for the nonlinear system with $K_{22} = 0.01$, in steady-state, with the initial condition given by Eqs. (10) and (11).

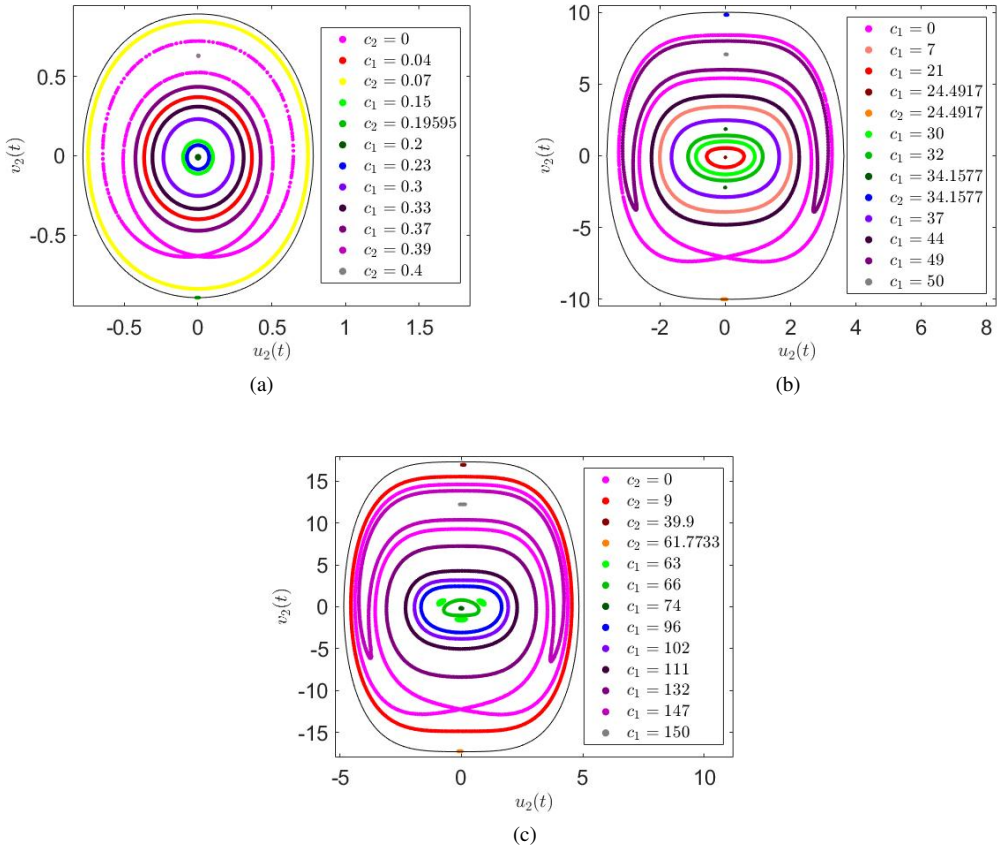

Figure 5: Poincaré map for the spring-mass nonlinear system with $K_{22} = 0.01$. The variables c_1 e c_2 are analyzed within the interval of 0 to h. a) $h = 0.4$, b) $h = 50$ and c) $h = 150$.

At Fig. 5a, the system has low energy ($h = 0.4$) and there are 3 stable NMs ($c_2 = 0.19595$, $c_1 = 0.2$ and $c_2 = 0.4$) and 1 unstable NM ($c_2 = 0$). Figure 5b shows the Poincaré map for intermediate energy ($h = 50$), where the system has 4 stable NMs ($c_1 = 24.4917$, $c_2 = 24.4917$, $c_2 = 34.1577$ and $c_1 = 50$) and 1 unstable NM ($c_1 = 0$). The map for $c_1 = 34.1577$ has 2 points and it is not considered a mode, seeing that the definition of Rosenberg (1962) is used, in other words, for a synchronous time response, the Poincaré map must be just one single point. At Fig. 5c, for high energies ($h = 150$), the system has 4 stable modes ($c_2 = 39.9$, $c = 61.7733$, $c_1 = 74$ and $c_1 = 150$) and 1 unstable NM ($c_2 = 0$), with 5 modes in total.

5.2 Second Case ($K_{22} = 0.1$)

Figure 6 displays the Poincaré map for the nonlinear system with $K_{22} = 0.1$, with the system in steady-state and with the initial condition given by Eqs. (10) and (11).

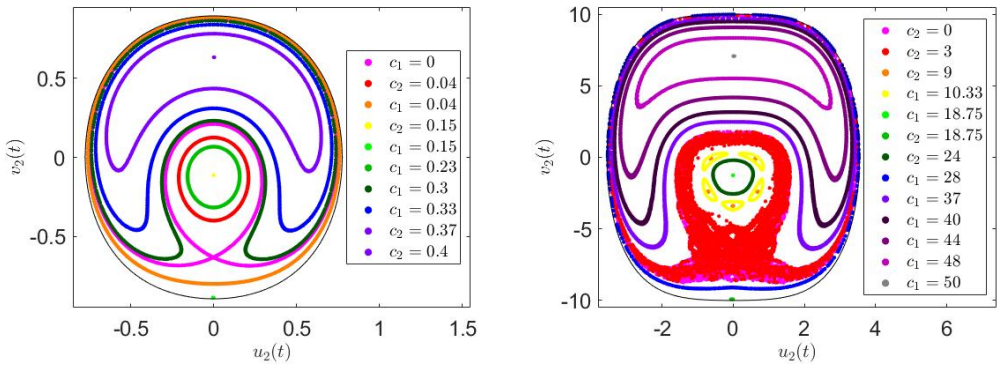

(a)

(b)

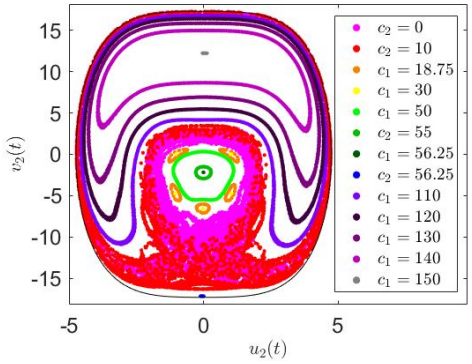

(c)

Figure 6: Poincaré map for the spring-mass nonlinear system with $K_{22} = 0.1$. The variables c_1 e c_2 are analyzed within the interval of 0 to h. a) $h = 0.4$, b) $h = 50$ and c) $h = 150$.

Figures 6a, 6b and 6c are the same from the ones obtained by Vakakis and Rand (1992a) and Vakakis and Rand (1992b). Thus, the computational program used in this work is validated. At Fig. 6a, for $h = 0.4$, there are 3 stable NMs ($c_1 = 0.15$, $c_2 = 0.15$ and $c_2 = 0.4$) and 1 unstable NM ($c_2 = 0$). At Fig. 6b, the energy is increase to the level $h = 50$ and one can note 3 stable NMs ($c_1 = 18.75$, $c_2 = 18.75$ and $c_1 = 50$). Furthermore, there is a dense region at $c_2 = 0$, which indicates qualitatively chaotic motion from the system. Figure 6c shows the results for a even higher energy ($h = 150$) and 3 stable NMs can be seen ($c_1 = 56.25$, $c_2 = 56.25$ and $c_1 = 150$). Once more, there is a chaotic like motion for two values ($c_2 = 0$ and $c_2 = 10$). Lichtenberg and Lieberman (2013) describe this dense region as a "stochastic sea", since it looks like a random map. Although the chaos may seem random, it is a deterministic behavior, once there is no random elements in the system.

5.3 Third Case ($K_{22} = 1$)

Figure 7 shows the Poincaré map for the nonlinear system with $K_{22} = 1$, with the system in steady-state and the initial condition given by Eqs. (10) and (11).

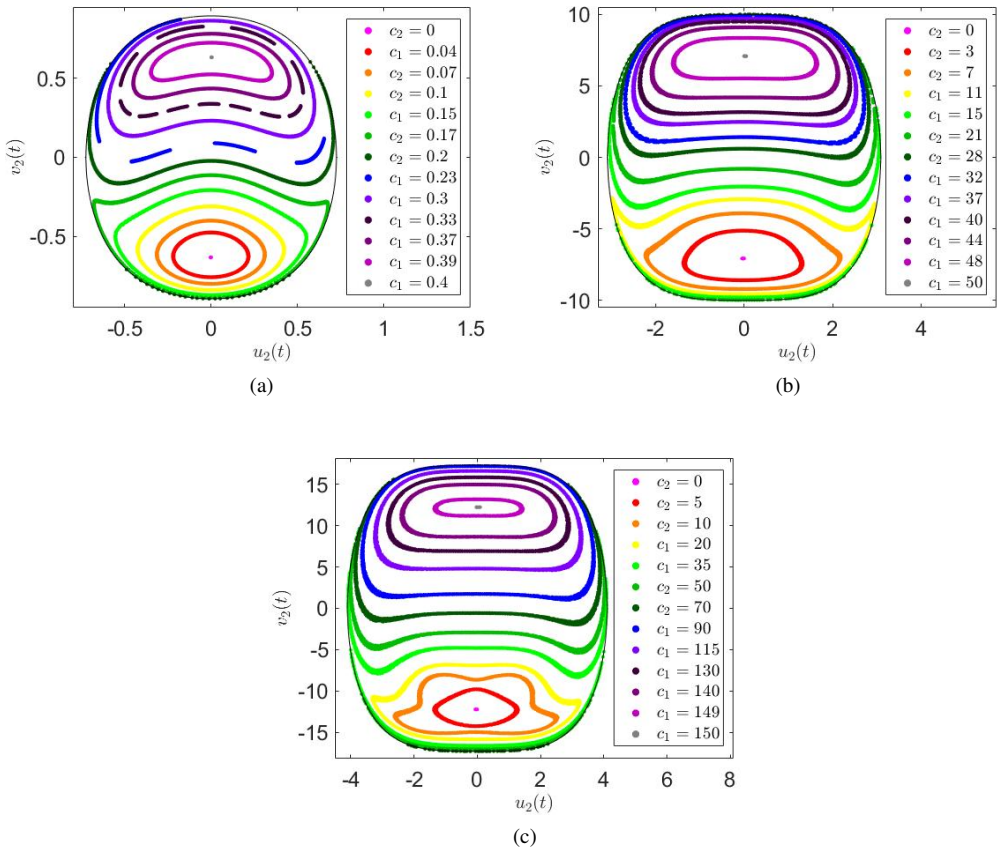

Figure 7: Poincaré map for the spring-mass nonlinear system with $K_{22} = 1$. The variables c_1 e c_2 are analyzed within the interval of 0 to h. a) $h = 0.4$, b) $h = 50$ and c) $h = 150$.

At Fig. 7a, the system has low energy ($h = 0.4$) and there are only 2 stable NMs ($c_2 = 0$ and $c_1 = 0.4$). At Fig. 7b, for $h = 50$, there are 2 stable modes ($c_2 = 0$ and $c_1 = 50$). Figure 7c displays the Poincaré map with $h = 150$ and, once again, only 2 stable NMs are present ($c_2 = 0$ and $c_1 = 150$). The system with $K_{22} = 1$ is similar to a linear system, seeing that the number of modes is equal to the number of DOFs for all the 3 levels of energy analyzed.

5.4 Fourth Case ($K_{22} = 10$)

Figure 8 displays the Poincaré map for the nonlinear system with $K_{22} = 10$, with the system in steady-state and the initial condition given by Eqs. (10) and (11).

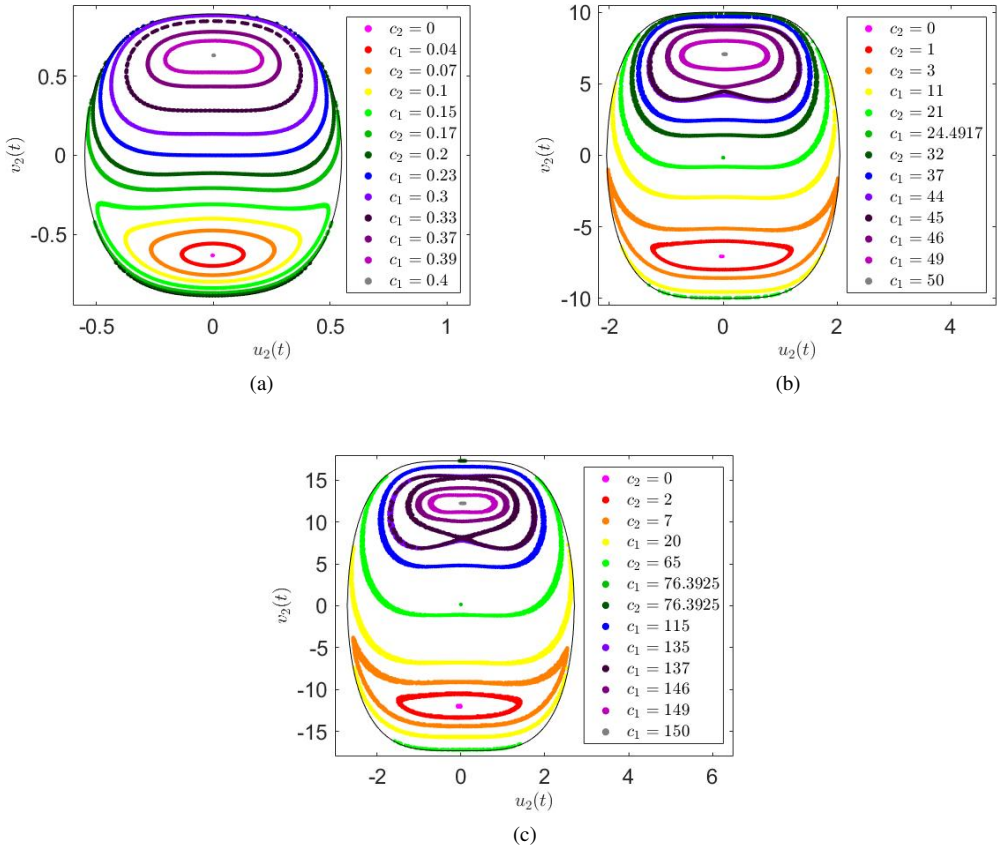

Figure 8: Poincaré map for the spring-mass nonlinear system with $K_{22} = 10$. The variables c_1 e c_2 are analyzed within the interval of 0 to h. a) $h = 0.4$, b) $h = 50$ and c) $h = 150$.

At Fig. 8a, for $h = 0.4$, there are 2 stable NMs ($c_2 = 0$ and $c_1 = 0.4$). Figure 8b displays the Poincaré map for $h = 50$ with 3 stable NMs ($c_2 = 0$, $c_1 = 45$ e $c_1 = 50$) and 1 unstable NM ($c_1 = 24.4917$). At Fig. 8c, for $h = 150$, there are 4 stable NMs ($c_2 = 0$, $c_1 = 76.3925$ e $c_2 = 76.3925$ and $c_1 = 150$) and 1 unstable NM ($c_1 = 137$), with 5 modes in total.

5.5 Result's Summary

A summary of each behavior from the 4 different cases is presented at Tab. 1.

Table 1: Number of NMs, their stability and indication of chaotic motion for different values of energy, h, and nonlinear stiffness, K_{22}.

	$h = 0.4$	$h = 50$	$h = 150$
$K_{22} = 0.01$	3 stable NMs 1 unstable NM	4 stable NMs 1 unstable NM	4 stable NMs 1 unstable NM
$K_{22} = 0.1$	3 stable NMs 1 unstable NM	3 stable NMs chaotic region	3 stable NMs chaotic region
$K_{22} = 1$	2 stable NMs	2 stable NMs	2 stable NMs
$K_{22} = 10$	2 stable NMs	3 stable NMs 1 unstable NM	4 stable NMs 1 unstable NM

At Tab. 1, the chaotic region only appeared for the system with $K_{22} = 0.1$ and for the energies $h = 50$ and $h = 150$. For a low energy of $h = 0.4$, the region was not present, since chaotic behavior is related to high energies (Vakakis and Rand, 1992b). Furthermore, one can note that, for $K_{22} = 1$, the system has 2 NMs for all 3 energy values, which resembles the behavior of a linear system, since the number of modes matched the number of DOFs and linear modes do not depend upon the variation of energy.

6. CONCLUSION

In this work, the NMs of a 2 DOFs system with nonlinear stiffness were identified with a qualitatively method. Besides that, a dense region was recognized, which indicates a chaotic behavior. A parametric analysis was carried out, as the quantity of modes was measured for different values of energy, h, and nonlinear stiffness, K_{22}.

From the results, the system 's level of total energy changes significantly the number of NMs. This dependency of the modes with the energy is not presented in linear systems. Overall, as the level of energy increases, the number of modes also increases or remains constant. The only exception is the system with $K_{22} = 0.1$, because the growth of energy level transformed an unstable NM into a possible chaotic motion. Furthermore, for the system with $K_{22} = 1$, the number of mode always remains equal to 2. Thus, the system presented a behavior similar to a linear system, seeing that the number of DOFs always matched the number of modes.

The technique based on the Poincaré can be used for identification of the NM defined by Rosenberg (1962), without the need for an analytic and extensive calculations.

7. ACKNOWLEDGMENTS

The authors would like to acknowledge the support of the Fundação de Apoio à Pesquisa do Distrito Federal (FAP-DF) and the Dynamic Systems Group (GDS) from the University of Brasília (UnB).

8. REFERENCES

Bengtsson, L., Ghil, M. and Källén, E., 1981. *Dynamic meteorology: data assimilation methods*, Vol. 330. Springer.

Costantino, R.F., Desharnais, R., Cushing, J.M. and Dennis, B., 1997. "Chaotic dynamics in an insect population". *Science*, Vol. 275, No. 5298, pp. 389–391.

Dinicola, S., D'Anselmi, F., Pasqualato, A., Proietti, S., Lisi, E., Cucina, A. and Bizzarri, M., 2011. "A systems biology approach to cancer: fractals, attractors, and nonlinear dynamics". *Omics: a journal of integrative biology*, Vol. 15, No. 3, pp. 93–104.

Gonçalves, P.B., 2012. *Aplicação dos modos de vibração não lineares a modelos conceituais de estruturas offshore*. Ph.D. thesis, PUC-Rio.

Kerschen, G., Peeters, M., Golinval, J.C. and Vakakis, A.F., 2009. "Nonlinear normal modes, part i: A useful framework for the structural dynamicist". *Mechanical systems and signal processing*, Vol. 23, No. 1, pp. 170–194.

Krishnaswami, G.S. and Senapati, H., 2019. "An introduction to the classical three-body problem". *Resonance*, Vol. 24, No. 1, pp. 87–114.

Lichtenberg, A.J. and Lieberman, M.A., 2013. *Regular and stochastic motion*, Vol. 38. Springer Science & Business Media.

Month, L.A. and Rand, R.H., 1980. "An application of the Poincaré map to the stability of nonlinear normal modes". *Journal of Applied Mechanics*, Vol. 47, No. 3, p. 645–651.

Rosenberg, R.M., 1962. "The normal modes of nonlinear n-degree-of-freedom systems". *Journal of Applied Mechanics*, Vol. 29, No. 1, pp. 7–14.

Rosenberg, R., 1966. "On nonlinear vibrations of systems with many degrees of freedom". In *Advances in applied mechanics*, Elsevier, Vol. 9, pp. 155–242.

Sastry, S., 2013. *Nonlinear systems: analysis, stability, and control*, Vol. 10. Springer Science & Business Media.

Savi, M.A., 2006. *Dinâmica não-linear e caos*. Editora E-papers.

Shaw, S.W. and Pierre, C., 1993. "Normal modes for non-linear vibratory systems". *Journal of sound and vibration*, Vol. 164, No. 1, pp. 85–124.

Vakakis, A.F. and Rand, R., 1992a. "Normal modes and global dynamics of a two-degree-of-freedom non-linear system—i. low energies". *International Journal of Non-Linear Mechanics*, Vol. 27, No. 5, pp. 861–874.

Vakakis, A.F. and Rand, R., 1992b. "Normal modes and global dynamics of a two-degree-of-freedom non-linear system—ii. high energies". *International Journal of Non-Linear Mechanics*, Vol. 27, No. 5, pp. 875–888.

9. RESPONSIBILITY NOTICE

The authors are solely responsible for the printed material included in this paper.